NJC
New Journal of Chemistry
A journal for new directions in chemistry

Accepted Manuscript

This article can be cited before page numbers have been issued, to do this please use: A. E. Sandeli, N. Khiri-Meribout, S. Benzerka, H. Boulebd, N. Gürbüz, N. Özdemir and . Özdemir, *New J. Chem.*, 2021, DOI: 10.1039/D1NJ03388C.

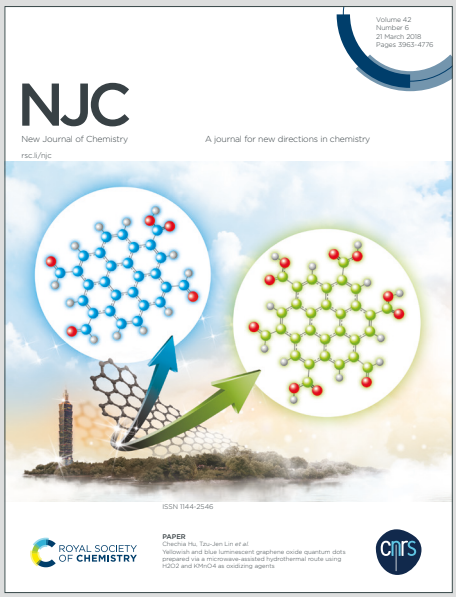

This is an Accepted Manuscript, which has been through the Royal Society of Chemistry peer review process and has been accepted for publication.

Accepted Manuscripts are published online shortly after acceptance, before technical editing, formatting and proof reading. Using this free service, authors can make their results available to the community, in citable form, before we publish the edited article. We will replace this Accepted Manuscript with the edited and formatted Advance Article as soon as it is available.

You can find more information about Accepted Manuscripts in the Information for Authors.

Please note that technical editing may introduce minor changes to the text and/or graphics, which may alter content. The journal's standard Terms & Conditions and the Ethical guidelines still apply. In no event shall the Royal Society of Chemistry be held responsible for any errors or omissions in this Accepted Manuscript or any consequences arising from the use of any information it contains.

View Article Online
DOI: 10.1039/D1NJ03388C

ARTICLE

Synthesis, structures, DFT calculations, and catalytic application in the direct arylation of five-membered heteroarenes with aryl bromides of novel Palladium-*N*-Heterocyclic carbene complexes PEPPSI-Type

Received 00th January 20xx,
Accepted 00th January 20xx

DOI: 10.1039/x0xx00000x

Abd el-Krim Sandeli,[a,d] Naima Khiri-Meribout,[a,b]* Saida Benzerka,[a,b] Houssem Boulebd,[a,b] Nevin Gürbüz,[c,d] Namık Özdemir,[e] and İsmail Özdemir[c,d]*

New series of Pd-catalysts based N-heterocyclic carbene ligand PEPPSI-Type, (PEPPSI = Pyridine Enhanced Precatalyst Preparation Stabilization and Initiation) with the general formula [Pd(II)Br2(NHC)(pyridine)] were synthesized, and fully characterized by spectroscopic analytical methods. Further, the structural characterization of **3a, 3b,** and **3d** was determined by a single-crystal X-ray diffraction study, which supports the proposed structures and offered a more detailed structural characterization. As well the result for representative molecule 3a has been confirmed on their electronic, vibrational, thermodynamic, and optical properties utilizing Density Functional Theory (DFT) calculations. The experimental molecular geometry of the ground state of complex 3a has been compared with the minimized structure obtained from DFT calculations. B3LYP functional in conjunction with LANL2DZ basis set for Palladium atom and 6-311G(d,p) basis set for hydrogen, carbon, nitrogen, and bromine atoms have been used for all calculations. Frontier molecular orbitals and molecular electrostatic potential were also analyzed and discussed. Due to the big interest in halo substituted arylated heteroarenes in organic chemistry. The capacity catalytic of these Pd(II)-NHC complexes PEPPSI – Type were evaluated by the direct arylation process of five-membered heteroaromatics such as thiophene, furan, and thiazole derivatives with various (hetero)aryl bromides in the presence of 1 mol% catalyst. The results showed that all new Pd-NHC complexes are effective catalysts that exhibit very good catalytic activity and gave C-H activation selectively at the C(5)-position of 2-acetyl furan and 2-acetyl thiophene.

Introduction

N-Heterocyclic carbenes (NHC) are effective ligands that allow the preparation of the most metal complexes, and chemically acceptable catalysts by altering the substituents on the nitrogen atom.[1] They have become one of the most widely used ligand classes in organometallic chemistry with new catalytic applications. Due to the activity, stability, and selectivity of metal complexes containing NHC ligand, they have been widely used as highly reactive and rather selective catalysts for a lot of reactions.[2] Over the last few decades, considerable advances have been achieved in direct arylation methods. Various transition metals such as Pd, Ru, Rh, etc, are effective for the direct arylation reactions.[3] However, among them, the Pd-complexes are the most powerful. Today, palladium-catalyzed cross-coupling reactions are highly important synthetic tools in organic chemistry.[4] Due to these features, they have been successfully employed in different applications of organometallic chemistry as a key ligand for metal complexes.[5] We can categorize the most used Pd-NHC complexes into four main classes; bis-Pd-NHCs, allyl-type Pd-NHCs, incer-type Pd-NHCs, and **PEPPSI** (**P**yridine **E**nhanced **P**re-catalyst **P**reparation **S**tabilization and **I**nitiation) type Pd-NHCs[6,7] Among the most popular catalysts for such reactions are PEPPSI-type palladium-NHC complexes of the type [PdX_2(NHC)(pyridine)] (X/halide) which have gained real practical importance in various catalytic processes.

The direct arylation of heteroarenes is particularly attractive since these moieties are present in many biologically active compounds. In recent years, Pd-catalyzed direct arylation of (hetero)arenes with (pseudo)halides have received significant attention as eco-friendly and economic alternatives to conventional methods. They consider as the most commonly employed coupling partners for Pd-catalyzed direct arylation reactions.[8] In 1985-1992, Ohta et al. first reported the direct

[a] *Research Laboratory of Synthesis of Molecules with Biological Interest, Mentouri Constantine-1 University, CONSTANTINE, ALGERIA*
[b] *Faculty of Science, Department of Chemistry, Mentouri Constantine-1 University, CONSTANTINE, ALGERIA*
[c] *Faculty of Science and Art, Department of Chemistry, İnönü University, MALATYA, TURKEY*
[d] *Catalysis Research and Application Center, Inönü University, 44280 MALATYA, TURKEY*
[e] *Department of Mathematics and Science Education, Faculty of Education, Ondokuz Mayıs University, 55139 SAMSUN, TURKEY*
† *Dedicated to Prof. Christian Bruneau for his outstanding contribution to organometallic chemistryc atalysis*
Electronic Supplementary Information (ESI) available: [details of any supplementary information available should be included here]. See DOI: 10.1039/x0xx00000x

View Article Online DOI: 10.1039/D1NJ03389C

arylation of heteroaromatics with aryl halides using a C-H activation strategy through the cleavage of two C-H bonds, which $Pd(PPh_3)_4$ was used as the catalyst and dimethylacetamide (DMAc) as the solvent.[9-11] After Organ et al[3] reported easily handled, air- and moisture-stable Pd–NHC complexes created by using the PEPPSI method, which featured Pd(II) species bearing an NHC ligand, two halides, and a labile ligand such as 3-chloropyridine. Following the discovery of Organ's PEPPSI-type Pd-complexes, which considers a new class of Pd-catalysts that are completely different from other Pd–NHC complexes and easier to synthesize and use.[12] This type of complex has shown remarkable catalytic activities towards various carbon-carbon and carbon-heteroatom coupling reactions. In recent years some studies on the direct arylation reaction of PEPPSI type palladium-N-heterocyclic carbene (NHC) complexes have been, published.[13,14] The researchers synthesized Pd-NHC complexes which contained different imidazole,[15] benzimidazole[16] and benzotriazole. In the last two decades, PEPPSI-themed Pd-complexes have been used as effective catalysts in direct arylation and successful results have been obtained.[17] Direct arylation reactions have received great interest as possible alternatives to the most employed cross-coupling reactions. Since then, palladium-catalyzed direct arylation has been successfully applied for the arylation of heteroaryl derivatives with aryl-halides has proved to be a powerful method for the synthesis of a wide variety of arylated heterocycles.[18-22] Very exciting results have been reported by several groups using thiophenes, furans, pyrroles, thiazoles, oxazoles, imidazoles, or triazoles.[23,24] Azole-derived metal complexes have found application in many fields.[25-27] In particular, nucleophilic N-heterocyclic carbenes (NHCs) have proven as useful ligands for transition metal catalysis.[28-30] In another way both thiophene and thiazole derivatives have attracted attention due to their important biological activity such as Sulfathiazole is an antimicrobial drug, 2-arylthiophene derivative Canagliflozin is a drug used in the treatment of type 2 diabetes, Atliprofen is an anti-inflammatory drug, Motapizone is used in the treatment against platelet aggregation diabetes, and Tiemonium is antimuscarinics.[31-33] Several thiophene derivatives containing a hydroxyalkyl group at C2 have also been found to be bioactive. Duloxetine is employed against major depressive disorder and penthienate is antimuscarinic; also several 2-arylated furans display important biological properties. For example, Dantrolene is a muscle relaxant and lapatinib is employed against breast cancer (Figure 1).

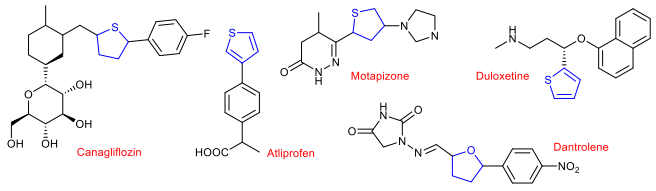

Figure 1. Examples of bioactive thiazole, thiophene, and furan derivatives.

Since they have such important biological activity, the discovery of more direct and selective procedures to synthesize arylated thiophene, thiazole, and furan derivatives is an important topic in synthetic organic chemistry. The use of such functional halo thiophenes for direct arylation would be useful, as they would give simple access to a wide variety of polyfunctionalized thiophenes useful for material chemistry or pharmaceutical applications. In this context, recently in an attempt to provide a new vision of the topic, we report the successful synthesis of six new PEPPSI-Type Pd(II)-NHC complexes (**3a–3e**) of the general formula [PdX2(NHC)(pyridine)], (X=Br; NHC=1,3-disubstituted 3,5-dimethylbenzimidazole-2-ylidene). In the present study, we have focused our attention on their applications in catalytic processes paying special investigation on the catalytic activity of all these newly synthesized Pd(II)-NHC complexes in direct C5 arylation reactions of a variety of five-membered heteroarenes such as 2- acetylfuran, 2-acetylthiophene, and furaldehyde with several aryl bromides in the presence of 1 mol% catalyst loading.

Experimental

All manipulations were performed in Schlenk-type flasks under an argon atmosphere. The melting point measurements were determined in open capillary tubes with an Electrothermal-9200 melting points apparatus. The IR spectra were recorded on the Gladi ATR unit (Attenuated Total Reflection) in the range of 450-4000 cm^{-1} with a Perkin Elmer Spectrum 100 Fourier-transform infrared spectrometer. Routine ^1H NMR and ^{13}C NMR spectra were recorded with a Bruker Ascend™ 400 Avance III HD NMR spectrometer with sample solutions prepared in $CDCl_3$. The chemical shifts (δ) were reported in parts per million (ppm) relative to tetramethylsilane (TMS) as an internal standard. Coupling constants (J values) were given in hertz (Hz). NMR multiplicities were abbreviated as follows: s = singlet, d = doublet, t = triplet, hept = heptet, dd = doublet of doublets, m = multiplet. ^1H NMR spectra were referenced to residual protiated solvents (δ = 7.28 ppm for $CDCl_3$), ^{13}C NMR chemical shifts were reported relative to deuterated solvents (δ = 77.16 ppm for $CDCl_3$). The catalytic solutions were analyzed with a Shimadzu GC 2025 equipped with a GC-FID sensor and RX-5ms column of 30 m length, 0.25 mm diameter and 0.25 µm film thickness. All the measurements were taken at room temperature for freshly prepared solutions.

General procedure for the preparation of benzimidazolium salts (2a-e)

A mixture of 1-benzhydryl-5,6-dimethyl-benzimidazole (1 mmol) and an equivalent amount of alkyl halide derivative (1 mmol), in degassed dimethylformamide. The reaction mixture was heated and stirred at 80 °C for 48h under argon. The obtained mixture was cooled at room temperature, After completion of the reaction, 45 mL of ether were added, and stirred for 1h, then the product filtered and washed with diethyl ether to remove the impurities, and the product was left

precipitated with high purity. After, the crude products were recrystallized in dichloromethane and dried under vacuum to provide pure products for experimental analysis. All benzimidazolium salts (**2a-e**) were isolated as air- and moisture-stable white solids in high yields. For the ^{1}H NMR, ^{13}C NMR, and FT-IR spectrums of the benzimidazolium salts. All benzimidazolium salts were published in our previous study.[34]

General procedure for the preparation of the PEPPSI-type Pd(II)-NHC complexes (3a-e)

The palladium(II)-NHC complexes PEPPSI-type could be synthesized by the interaction of benzimidazolium salts with $PdCl_2$ (1mmol) and pyridine in the presence of potassium carbonate K_2CO_3 (5mmol). After the addition of KBr (10 mmol) solution was stirred and heated for 48 h at 80 °C. The reactions were carried out in acetonitrile (15 mL) under an atmosphere of nitrogen. The solvent was removed under vacuum to afford the product and eliminate pyridine then the mixture was washed with hexane three times. The black solid formed was dissolved in DCM (CH_2Cl_2) and purified by a flash column chromatography on silica gel, eluting with DCM until the product was completely recovered. DCM was removed under reduced pressure and the pure complex was obtained as a yellow powder solid. Further, The crude product was recrystallized from dichloromethane: hexane (1:6), to get pure complexes for analysis and catalysis. The palladium complexes, which are highly moisture- and air-stable both in solution and solid-state against air, light and moisture.

Dibromo[1-benzhydryl-5,6-dimethyl-3-(4-methylbenzyl)benzimedazole-2-ylidene]pyridine palladium (II), 3a

Yield 71%; 150 mg; m.p: 292-293°C; yellow-solid(crystal); FT-IR ν(CN)=1400cm^{-1} .^{1}H-NMR (400MHz, $CDCl_3$, TMS, 25°C): δ(ppm) = 8.98 (d, *J* =5.0 Hz, 2H, $NC_5\underline{H}_5$); 8.58 (s, 1H, N-$C_6\underline{H}_2(CH_3)_2$-N); 7.72 (t, *J* =7.6 Hz, 1H, $C_5\underline{H}_5$); 7.51 (d, *J* =8.1 Hz, 2H, N-$C_6\underline{H}_4(CH_3)$-N); 7.48 (d, *J* =8.6 Hz, 4H, C<u>H</u>-Ar); 7.32-7.27 (m, 6H, C<u>H</u>-Ar); 7.18 (d, *J* =8.1 Hz, 2H, N-$C_6\underline{H}_4(CH_3)$-N); 6.82 (s, 1H, N-$C_6\underline{H}_2(CH_3)_2$-N); 6.45 (s, 1H, Ph-C<u>H</u>-Ph); 6.14 (s, 2H, $NC\underline{H}_2$-$C_6H_4(CH_3)$); 2.34 (s, 3H, $C\underline{H}_3$); 2.14 (s, 3H, $C\underline{H}_3$); 2.02 (s, 3H, $C\underline{H}_3$). ^{13}C-NMR (400MHz, $CDCl_3$, TMS, 25°C): δ(ppm) = 20.13 ($\underline{C}H_3$,C_5); 20.25 ($\underline{C}H_3$,C_7); 21.22 ($\underline{C}H_3$,C_{15}); 53.42 (N-$\underline{C}H_2$,C_{10}); 67,97 (Ph-$\underline{C}$H-Ph,C_{18}); 111.75 ($\underline{C}$H,C_8); 113.73 ($\underline{C}$H,C_3); 124.46 ($\underline{C}$H, N$\underline{C}_5H_5$,$C_{32,34}$); 127.94 (2$\underline{C}$H,$C_{22,28}$); 128.01 (2$\underline{C}$H,$C_{13,16}$); 128.44 (4$\underline{C}$H,$C_{20,24,26,30}$); 129.18 (4$\underline{C}$H,$C_{21,23,27,29}$); 129.47 (2$\underline{C}$H, $C_{12,17}$); 131.84 (C_{11}); 131.97 (C_9); 132.05 (C_2); 133.15 (C_6); 133.57 (C_4); 137.68 ($\underline{C}$H, N$\underline{C}_5H_5$,C_{33}); 137.74 ($C_{19,25}$); 137.78 (C_{14}); 152.65 (N$\underline{C}_5H_5$,$C_{31,35}$); 163.38 (Pd-*C*carb,C_1). Elemental analysis calcd. (%) for $C_{35}H_{33}Br_2N_3Pd$ (M.w.= 761.90 g/mol): C 55.18, H 4.37, N 5.52; found (%): C 54.98, H 4.43, N 5.37.

Dibromo[1-benzhydryl-5,6-dimethyl-3-(2,3,5,6-tetramethylbenzyl)-benzimedazole-2-ylidene]pyridinepalladium (II), 3b

Yield 85%; 215 mg; m.p: 244-245 °C; yellow-solid(crystal); FT-IR ν(CN)=1400 cm^{-1} .^{1}H-NMR (400MHz, $CDCl_3$, TMS, 25°C): δ(ppm) = 8.91 (d, *J* =5.0 Hz, 2H, $NC_5\underline{H}_5$); 8.60 (s, 1H, N-$C_6\underline{H}_2(CH_3)_2$-N); 7.70 (t, *J* =7.6 Hz, 1H, $NC_5\underline{H}_5$); 7.46 (d, *J* =6.7 Hz , 4H, CH-Ar); 7.35 (m, 6H, CH-Ar); 7.29 (t, *J* =7.6 Hz, 2H, $NC_5\underline{H}_5$); 7.10 (s, 1H, N-$C_6\underline{H}_2(CH_3)_2$-N); 6.46 (s, 1H, Ph-C<u>H</u>-Ph); 6.17 (s, 2H, NCH_2-$C_6H_1(CH_3)_4$); 6.13 (s, 1H, $C_6\underline{H}_1(CH_3)_4$); 2.29 (s, 6H, $C\underline{H}_3$); 2.28 (s, 6H, $C\underline{H}_3$); 2.01 (s, 3H, $C\underline{H}_3$); 2.00 (s, 3H, $C\underline{H}_3$). ^{13}C-NMR (400MHz, $CDCl_3$, TMS, 25°C): δ(ppm) = 16.82 (2$\underline{C}H_3$,$C_{13,20}$); 20.13 ($\underline{C}H_3$,C_5); 20.28 ($\underline{C}H_3$,C_7); 20.60 (2$\underline{C}H_3$,$C_{15,18}$); 51.19 (N-$\underline{C}H_2$,C_{10}); 68,05 (Ph-$\underline{C}$H-Ph,C_{21}); 111.74 ($\underline{C}$H,C_8); 113.50 ($\underline{C}$H,C_3); 124.21 ($\underline{C}$H, N$\underline{C}_5H_5$,$C_{35,37}$); 127.91 (2$\underline{C}$H,$C_{25,31}$); 128.40 (4$\underline{C}$H,$C_{23,27,29,33}$); 129.15 (4$\underline{C}$H,$C_{24,26,30,32}$); 130.84 (C_{11}); 131.26 (C_9); 131.50 (C_2); 132.35 (C_6); 132.88 (C_4); 134.23 ($C_{12,19}$); 135.18($C_{14,17}$); 137.69 ($\underline{C}$H, N$\underline{C}_5H_5$,C_{36}); 137.85 (C<u>H</u>,$C_{22,28}$); 152.56 (N$\underline{C}_5H_5$,$C_{34,38}$); 163.18 (Pd-*C*carb,C_1). Elemental analysis calcd. (%) for $C_{38}H_{39}Br_2N3Pd$ (M.w.= 803.98 g/mol): C 56.77, H 4.89, N 4.54; found (%): C 56.85, H 4.58, N 4.90.

Dibromo[1-benzhydryl-5,6-dimethyl-3-(2,4,6-trimethylbenzyl)benzimedazole-2-ylidene]pyridinepalladium (II), 3c

Yield 81%; 130 mg; m.p: 153-154 °C; yellow-solid(crystal); FT-IR ν(CN)=1400 cm^{-1} .^{1}H-NMR (400MHz, $CDCl_3$, TMS, 25°C): δ(ppm) = 8.96 (d, *J* =5.2 Hz, 2H, $NC_5\underline{H}_5$); 8.60 (s, 1H, N-$C_6\underline{H}_2(CH_3)_2$-N); 7.72 (t, *J* =7.7 Hz, 1H, $NC_5\underline{H}_5$); 7.46 (d, *J* =6.6 Hz, 4H, C<u>H</u>-Ar); 7.36 (m, 6H, C<u>H</u>-Ar); 7.30 (t, *J* =7.6 Hz, 2H, $NC_5\underline{H}_5$); 6.95 (s, 2H, $C_6\underline{H}_2(CH_3)_3$); 6.46 (s, 1H, Ph-C<u>H</u>-Ph); 6.14 (s, 2H, $NC\underline{H}_2$-$C_6H_2(CH_3)_3$); 6.13 (s, 1H, N-$C_6\underline{H}_2(CH_3)_2$-N); 2.38 (s, 6H, $C\underline{H}_3$); 2.35 (s, 3H, $C\underline{H}_3$); 2.00 (s, 3H, $C\underline{H}_3$); 1.99 (s, 3H, $C\underline{H}_3$). ^{13}C-NMR (400MHz, $CDCl_3$, TMS, 25°C): δ(ppm) = 20.13 (2C, $\underline{C}H_3$); 20.27 ($\underline{C}H_3$,C_5); 20.28 ($\underline{C}H_3$,C_7); 21.16 (2$\underline{C}H_3$,$C_{13,19}$); 22.66 ($\underline{C}H_3$,C_{16}); 50.79 (N-$\underline{C}H_2$,C_{10}); 68,00 (Ph-$\underline{C}$H-Ph,C_{20}); 111.68 ($\underline{C}$H,C_8); 113.53 ($\underline{C}$H,C_3); 124.44 ($\underline{C}$H, N$\underline{C}_5H_5$,$C_{34,36}$); 127.91(C_{11}); 127.94 (2$\underline{C}$H,$C_{24,30}$); 128.40 (4$\underline{C}$H,$C_{22,26,28,32}$); 129.13 (4$\underline{C}$H,$C_{23,25,29,31}$); 129.45 (2$\underline{C}$H,$C_{14,17}$); 131.36 (C_9); 131.60 (C_2); 132.95 (C_4); 134.05 (C_6); 137.74 ($\underline{C}$H, N$\underline{C}_5H_5$,C_{35}); 137.82 ($C_{21,27}$); 138.48(C_{15}); 138.92($C_{12,18}$); 152.61 (N$\underline{C}_5H_5$,$C_{33,37}$); 163.18 (Pd-*C*carb,C_1). Elemental analysis calcd. (%) for $C_{37}H_{37}Br_2N_3Pd$ (M.w.= 789.95 g/mol): C 55.26, H 4.72, N 5.32; found (%): C 55.56, H 4.67, N 5.15.

Dibromo[1-benzhydryl-5,6-dimethyl-3-(3,4,5-trimethoxybenzyl)benzimedazol-2-ylidene]pyridinepalladium (II), 3d

Yield 69%; 220 mg; m.p: 264-265 °C; yellow-solid(crystal); FT-IR ν(CN)=1404 cm^{-1} .^{1}H-NMR (400MHz, $CDCl_3$, TMS, 25°C): δ(ppm) = 8.99 (d, *J* =5.2 Hz, 2H, $NC_5\underline{H}_5$); 8.58 (s, 1H, N-$C_6\underline{H}_2(CH_3)_2$-N); 7.72 (t, *J* =7.6 Hz, 1H, $NC_5\underline{H}_5$); 7.47 (d, *J* =5.3 Hz, 4H, C<u>H</u>-Ar); 7.35-7.37 (m, 6H, C<u>H</u>-Ar); 7.30 (t, *J* =7.6 Hz, 2H, $NC_5\underline{H}_5$); 6.90 (s, 2H, $C_6\underline{H}_2$-$(OCH_3)_3$); 6.88 (s, 1H, s, 1H, N-$C_6\underline{H}_2(CH_3)_2$-N); 6.46 (s, 1H, Ph-C<u>H</u>-Ph); 6.09 (s, 2H, $NC\underline{H}_2$-$C_6H_2(OCH_3)_3$); 3.87 (s, 6H, $OC\underline{H}_3$); 3.84 (s, 3H, $OC\underline{H}_3$); 2.17 (s, 3H, $C\underline{H}_3$); 2.04 (s, 3H, $C\underline{H}_3$). ^{13}C-NMR (400MHz, $CDCl_3$, TMS, 25°C): δ(ppm) = 20.20 ($\underline{C}H_3$,C_5); 20.27 ($\underline{C}H_3$,C_7); 53.79 (N-$\underline{C}H_2$,C_{10}); 56.69 (2O$\underline{C}H_3$,$C_{14,18}$); 60.85 (O$\underline{C}H_3$,C_{16}); 67,94 (Ph-$\underline{C}$H-Ph,C_{20}); 111.70 ($\underline{C}$H,C_8); 113.78 ($\underline{C}$H,C_3); 124.58 ($\underline{C}$H, N$\underline{C}_5H_5$,$C_{34,36}$); 125.37 (2$\underline{C}$H,$C_{12,19}$); 128.07 (2$\underline{C}$H,$C_{24,30}$); 128.44 (4$\underline{C}$H,$C_{22,26,28,32}$); 129.14 (4$\underline{C}$H,$C_{23,25,29,31}$); 131.83 (C_{11}); 131.94 (C_9); 132.05 (C_2); 133.15 (C_4); 133.58 (C_6); 137.62 (C_{15}); 137.68($C_{21,27}$); 137.85($\underline{C}$H, N$\underline{C}_5H_5$,C_{35}); 150.89 ($C_{13,17}$); 152.65 (N$\underline{C}_5H_5$,$C_{33,37}$); 163.29 (Pd-*C*carb,C_1). Elemental analysis calcd. (%) for $C_{37}H_{37}Br_2N_3O_3Pd$ (M.w.= 837.95 g/mol): C 53.04, H 4.45, N 5.01; found (%): C 52.81, H 4.27, N 5.04.

View Article Online DOI: 10.1039/D1NJ03788C

Dibromo[1-benzhydryl-5,6-dimethyl-3-(*4-tert-butylbenzyl*)benzimedazole-2-ylidene]pyridinepalladium (II), 3e

Yield 98%; 100 mg; 3.p: 276-277 °C; yellow-solid(crystal); FT-IR ν(CN)=1399cm^{-1} .^{1}H-NMR (400MHz, $CDCl_3$, TMS, 25°C): δ(ppm) = 8.98 (d, *J* =5.1 Hz, 2H, $NC_5\underline{H}_5$); 8.59 (s, 1H, N-$C_6\underline{H}_2(CH_3)_2$-N); 7.71 (t, *J* =7.7 Hz, 1H, $NC_5\underline{H}_5$); 7.57 (d, *J* =8.2 Hz, 2H, $C_6\underline{H}_4$-(tBu)); 7.49 (d, *J* =6.7 Hz, 4H, C<u>H</u>-Ar); 7.40 (d, *J* =8.2 Hz, 2H, $C_6\underline{H}_4$-(tBu)); 7.35 (m, 6H, C<u>H</u>-Ar); 7.29 (t, *J* =7.6 Hz, 2H, $NC_5\underline{H}_5$)6.82 (s, 2H, N-$C_6\underline{H}_2(CH_3)_2$-N); 6.45 (s, 1H, Ph-C<u>H</u>-Ph); 6.15 (s, 2H, $NC\underline{H}_2$-C_6H_4(tBu)); 2.14 (s, 3H, $C\underline{H}_3$); 2.03 (s, 3H, $C\underline{H}_3$); 1.31 (s, 9H, $C\underline{H}_3$/(tBu)). ^{13}C-NMR (400MHz, $CDCl_3$, TMS, 25°C): δ(ppm) = 20.08 ($\underline{C}H_3$,C_5); 20.25 ($\underline{C}H_3$,C_7); 31.33 (3$\underline{C}H_3$,$C_{16,17,18}$); 34.58 (<u>C</u>-$(CH_3)_3$, C_{15}); 53.37 (N-$\underline{C}H_2$,C_{10}); 67,95 (Ph-<u>C</u>H-Ph,C_{21}); 111.83 (<u>C</u>H,C_8); 113.72 (<u>C</u>H,C_3); 124.45 (<u>C</u>H, N$\underline{C}_5H_5$,$C_{35,37}$); 125.73 (2<u>C</u>H,$C_{23,19}$); 125.72 (2<u>C</u>H,$C_{24,30}$); 128.01 (2<u>C</u>H,$C_{12,20}$); 128.44 (4<u>C</u>H,$C_{23,27,29,33}$); 129.17 (4<u>C</u>H,$C_{24,26,30,32}$); 131.83 (C_{11}); 131.94 (C_9); 132.05 (C_2); 133.15 (C_4); 133.58 (C_6); 137.75 ($C_{22,28}$); 137.77 (<u>C</u>H, N$\underline{C}_5H_5$,C_{36}); 150.89(C_{14}); 152.65 (N$\underline{C}_5H_5$,$C_{34,38}$); 163.39 (Pd-*C*carb,C_1). Elemental analysis calcd. (%) for $C_{38}H_{39}Br_2N_3Pd$ (M.w.= 803.98 g/mol): C 56.77, H 4.89, N 5.23; found (%): C 56.43, H 4.71, N 5.16.

X-Ray crystallographic analysis study

The structure of Pd(II)-NHC complexes **3a**, **3b** and **3d** was determined by the X-ray diffraction technique, the obtained results confirmed all the spectroscopic data. A single Suitable crystal of complex **3a**, **3b** and **4d** for X-ray diffraction analysis was grown by slow diffusion of diethyl ether in a saturated chloroform solution at room temperature. Crystallographic data of **3a**, **3b** and **3d** were collected with an STOE IPDS II diffractometer at room temperature using graphite-monochromated Mo Kα radiation by applying the ω-scan method. Data collection and cell refinement were carried out using X-AREA while data reduction was applied using X-RED32[35] The structures were solved by direct methods with SIR2019[36] and refined through the full-matrix least-squares calculations on F^2 using SHELXL-2018[37] inserted in idealized positions and treated using a riding model, fixing the bond lengths at 0.93, 0.98, 0.97, and 0.96 Å for aromatic CH, methine CH, CH_2, and CH_3 atoms, respectively. The displacement parameters of the H atoms were fixed at U_{iso}(H) = 1.2U_{eq} (1.5U_{eq} for CH_3) of their parent atoms. The crystallographic data and refinement parameters are summarized in Table 1. Molecular graphics were generated by using OLEX2.[38]

Density Functional Theory (DFT) calculations

Computational details

All DFT (Density Functional Theory) calculations of this work have been performed using Gaussian09 software.[39] The B3LYP (Becke-Lee-Parr hybrid exchange-correlation three-parameter functional) functional[40,41] in conjunction with LANL2DZ[42] basis set for Palladium atom and 6-311G(d,p)[43] basis set for hydrogen, carbon, nitrogen, and bromine atoms have been used for all calculations. The B3LYP method is efficient for the prediction of molecular geometry and electronic properties and also offers a nice balance between cost and precision.[44-46] The ground state was validated by the absence of imaginary frequencies (no imaginary frequency).

Catalytic study of Pd(II)-NHC complexes PEPPSI-type

General Procedure for the direct arylation reaction

In 1990, the first examples of Pd-catalyzed direct arylation of furans and thiophenes were reported by Ohta.[10] In this pioneering work, the direct C(5)-arylation of furan, thiophene, and furaldehyde was carried out with electron-rich or electron-poor aryl bromides using [Pd(II)Br_2(*N*HC)(pyridine)] as the catalyst. In the last two decades, Pd-catalyzed direct arylation was successfully performed.[47-48] Therefore, in this catalysis study, we selected DMA as the solvent, and KOAc as the base according to the methods described in the literature.[49] In a typical experiment an oven-dried 10 mL Schlenk tube was charged with 1 mol% of Pd(II)-NHC complexes (0.01 mmol) as catalyst, five-membered heteroaromatic compound derivative (2.0 mmol), (hetero)aryl halide (1.0 mmol), KOAc (2.0 mmol) as a base, and DMAc (dimethylacetamide, 2 mL) as solvent under an argon atmosphere. The Schlenk tube was placed in a preheated oil bath at 120 °C, and the reaction mixture was stirred for 1h. After completion of the reaction, the solvent was removed under vacuum and the residue was solved with CH_2Cl_2 (2 mL) and charged directly onto a micro-silica gel chromatography column. The products were eluted by using *n*-hexane/diethyl ether mixture (5:1, v/v) as eluent to afford the pure product. The chemical characterizations of the products were checked by gas chromatography GC spectrometry. GC yields and Conversions were calculated by taking into account the conversion of aryl bromides to products from the results of GC spectrometry with dodecane as an internal standard.

Results and discussion

Preparation of PEPPSI-type palladium–NHC complexes 3a-e

The PEPPSI-themed Pd(II)-NHC complexes (**3a–e**) were synthesized according to procedures reported by Organ for other Pd–NHC–PEPPSI complexes.[21] All reactions for the preparation of the Palladium complexes were carried out under argon using standard Schlenk techniques. A solution of benzimidazolium salts (1eq), $PdCl_2$(1,5 eq.), in pyridine (2 eq.), K_2CO_3 (5 eq.) and a large excess of KBr(10 eq.), were dissolved in 15 mL of acetonitrile (15 mL) under an atmosphere of nitrogen. The reaction was stirred and heated for 02 days at 80 °C until the mixture becomes black. After the reaction was finished, the solvent was removed under vacuum to afford the product and eliminate pyridine then the mixture was washed with hexane three times. After removal of the hexane solvent, the residue was re-dissolved in CH_2Cl_2, filtered on a pad of silica covered with Celite, to remove unreacted $PdCl_2$. The crude product was obtained after evaporating the CH_2Cl_2 solvent. The crude product was recrystallized from dichloromethane: hexane (1:4). After chromatography on silica gel, the pure complex was obtained as a yellow Pd(II)-NHC complexes (**3a-e**) were obtained. All Pd(II)-NHC complexes were prepared in good yields through a simple procedure in a three-steps (Scheme 1)

View Article Online
DOI: 10.1039/D1NJ03388C

ARTICLE

from 5,6-dimethylbenzimidazole and benzhydryl reagents for the preparation of product 1 as a starting material, then the starting material reacts with various ligands of chlorobenzyl to obtain 5,6-dimethylbenzimidazoluim salts. These benzimidazolium salts **(2a-e)** were used as a precursor for the synthesis of Pd(II)-NHC complexes.

Table 1. Crystal data and structure refinement parameters for **3a, 3b,** and **3d**.

	Pd(II)-NHC complexes PEPPSI-Type		
Parameters	**3a**	**3b**	**3d**
CCDC depository	2073777	2073779	2073780
Color/shape	Yellow/prism	Yellow/prism	Yellow/prism
Chemical formula	$[PdBr_2(C_{30}H_{28}N_2)(C_5H_5N)]$	$[PdBr_2(C_{33}H_{34}N_2)(C_5H_5N)]$	$[PdBr_2(C_{32}H_{32}N_2O_3)(C_5H_5N)]$
Formula weight	761.86	803.94	837.91
Temperature (K)	296(2)	296(2)	296(2)
Wavelength (Å)	0.71073 Mo Kα	0.71073 Mo Kα	0.71073 Mo Kα
Crystal system	Monoclinic	Triclinic	Monoclinic
Space group	$P2_1/n$ (No. 14)	$P\bar{1}$ (No. 2)	$P\text{-}2_1/n$ (No. 14)
Unit cell parameters			
a, b, c (Å)	14.9802(13), 11.0510(7), 20.2398(15)	9.3043(7), 11.1447(9), 17.5332(14)	11.9557(9), 16.6440(8), 18.4136(13)
α, β, γ (°)	90, 106.685(6), 90	91.190(6), 104.973(6), 103.026(6)	90, 106.908(6), 90
Volume (Å^3)	3209.6(4)	1705.1(2)	3505.7(4)
Z	4	2	4
$D_{calc.}$ (g/cm^3)	1.577	1.566	1.588
μ (mm^{-1})	3.096	2.918	2.848
Absorption correction	Integration	Integration	Integration
$T_{min.}$, $T_{max.}$	0.5504, 0.8967	0.1567, 0.3154	0.2890, 0.7055
F_{000}	1520	808	1680
Crystal size (mm^3)	0.35 × 0.08 × 0.04	0.73 × 0.55 × 0.53	0.48 × 0.45 × 0.11
Diffractometer/measurement method	STOE IPDS II/ω scan	STOE IPDS II/ω scan	STOE IPDS II/ω scan
Index ranges	$-19 \le h \le 19$, $-14 \le k \le 14$, $-26 \le l \le 26$	$-12 \le h \le 12$, $-14 \le k \le 14$, $-22 \le l \le 22$	$-15 \le h \le 15$, $-21 \le k \le 19$, $-24 \le l \le 24$
ϑ range for data collection (°)	$1.993 \le \vartheta \le 27.956$	$1.882 \le \vartheta \le 27.802$	$1.683 \le \vartheta \le 27.737$
Reflections collected	36397	21039	54952
Independent/observed reflections	7650/3046	7945/4779	8206/6602
$R_{int.}$	0.2489	0.1482	0.0762
Refinement method	Full-matrix least-squares on F^2	Full-matrix least-squares on F^2	Full-matrix least-squares on F^2
Data/restraints/parameters	7650/0/373	7945/0/403	8206/0/420
Goodness-of-fit on F^2	0.972	1.036	1.165
Final R indices [$I > 2\sigma(I)$]	$R_1 = 0.0927$, $wR_2 = 0.1253$	$R_1 = 0.0771$, $wR_2 = 0.1750$	$R_1 = 0.0534$, w$R_2 = 0.0962$
R indices (all data)	$R_1 = 0.2310$, $wR_2 = 0.1641$	$R_1 = 0.1301$, $wR_2 = 0.2089$	$R_1 = 0.0727$, wR_2= 0.1022
$\Delta\rho_{max.}$, $\Delta\rho_{min.}$ (e/Å^3)	1.06, −0.69	1.17, −1.56	0.70, −0.56

View Article Online
DOI: 10.1039/D1NJ03388C

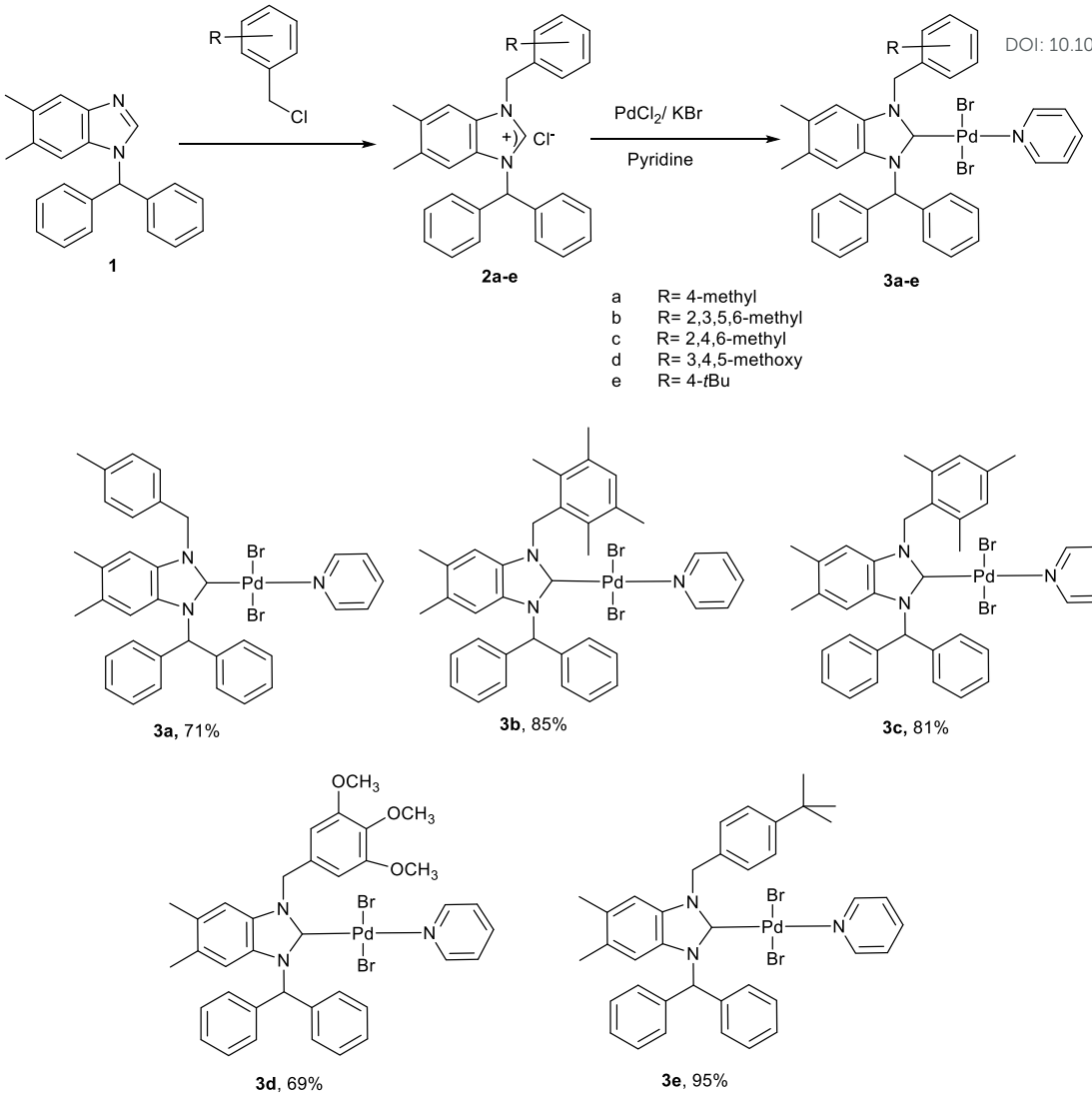

Scheme 1. Synthetic route and structure of Pd(II)-NHC complexes PEPPSI-type (**3a-e**).

All new five Pd(II)-NHC complexes 3a–e were showed good solubility in most organic solvents, such as chloroform, dichloromethane, ethanol, acetonitrile, and dimethylsulfoxide except non-polar ones, as pentane and hexane. They are highly moisture- and air-stable both in solution and in the solid-state against air, light, and moisture, which could be stored at room temperature for months without an obvious decline in catalytic efficiency. The new compounds were successfully characterized by spectroscopic techniques such as NMR, FT-IR, and elementary analysis to confirm the formation of the complexes. The physical and some spectroscopic data of Pd(II)-NHC complexes PEPPSI-type are summarized in Table 2. Firstly, the FT-IR spectroscopy data indicated that the PEPPSI-type Pd(II)-NHC complexes 3a-e exhibit a characteristic ν(CN) band typically at 1400, 1400, 1400, 1404 and 1399 cm^{-1} respectively. The formation of carbenes is correlated by a shift of the (CN) vibration. The FT-IR spectra of these five Pd (II)-NHC complexes show similar absorption bands. Due to the flow of electrons from the carbene ligand to the palladium center, the C=N bond is weakened, and as a result, a decrease in the *ν*(CN) stretching frequency is observed. Secondly, in the ^{1}H NMR the characteristic signals of aromatic hydrogens of pyridine ring were observed as downfield resonances in the ^{1}H NMR spectra in the d range of δ = 7.71-8.99 ppm. These signals suggest that the pyridine ring coordinated to the palladium centre to form a PEPPSI-type palladium complex. While in ^{13}C NMR the signals of the aromatic carbons of pyridine ring were detected at δ =152.65, 152.56, 152.61, 152.64, 152.65 ppm for the first two carbons CHNCH. While the second 2 carbons CH-CNC-CH were detected at δ =124.46, 124.21, 124.44, 124.58, 124.45 ppm, and δ =137.68, 137.69, 137.74, 137.85, 137.77 ppm for the carbon CHCHCH. All these data support the formation of the PEPPSI-type palladium complex. The PEPPSI Pd-NHC complexes were identified compared to benzimidazolium salts by a characteristic proton peak at the 2-position which not appeared as a signal of an acidic proton (NC*H*N) in the ^{1}H NMR and carbon peak in ^{13}C NMR (NC*H*N) spectra, the characteristic signals of the acidic proton and the benzimidazolium salts were not observed, which confirm the formation of Pd-carbene bond. The characteristic Pd–C_2-carbene signals of 3a-e complexes appear as a singlet at δ = 163.38, 163.18, 163.18, 163.29 and 163.39 ppm, respectively in ^{13}C NMR spectra. The elemental analysis results of these complexes are in agreement with the proposed molecular formula. These five new complexes show typical spectroscopic signatures, values are in

View Article Online
DOI: 10.1039/D1NJ03388C

agreement with reported data for similar PEPPSI type Pd(II)-NHC complexes.[14,49]

Table 2. Physical and some spectroscopic data of Pd(II)-NHC complexes PEPPSI-type

Code	Chemical Formula	Molecular Weight (g/mol)	Melting point °C	^{13}C NMR (C_2) ppm	IR $\nu_{(CN)}$
3a	$C_{35}H_{34}Br_2N_3Pd$	761,90	292-293	163,38	1400
3b	$C_{38}H_{40}Br_2N_3Pd$	803,98	244-245	163,18	1400
3c	$C_{37}H_{38}Br_2N_3Pd$	789,95	153-154	163,18	1400
3d	$C_{37}H_{38}Br_2N_3O_3Pd$	837,95	264-265	163,29	1404
3e	$C_{38}H_{40}Br_2N_3Pd$	803,98	276-277	163,39	1399

X-ray crystal structures

The solid-state structures of **3a**, **3b**, and **3d** with the adopted atom-labeling scheme are shown in Figs. 2-4, while important bond distances and angles are listed in Table 3. The palladium complexes are four-coordinated in a square-planar geometry and surrounded by the carbene carbon atom of the NHC ligand, the nitrogen atom of the pyridine ring, and two bromide atoms. The complexes have a slightly distorted square-planar geometry, in which the anion atoms are *trans* to each other. The *cis* angles varying from 85.32(19) to 93.23(17)° and the *trans* angles changing from 173.05(4) to 179.17(14)° deviate from their ideal values of 90 and 180°, respectively. For quantitative evaluation of the extent of distortion around the metal center, the structural indexes $\boldsymbol{\tau_4}$ [50] and $\boldsymbol{\tau_4'}$ [51] were employed; $\boldsymbol{\tau_4} = \frac{360°-(\alpha+\beta)}{360°-2\theta}$ $\boldsymbol{\tau_4'} = \frac{\beta-\alpha}{360°-\theta} + \frac{180°-\beta}{180°-\theta}$

where $\boldsymbol{\alpha}$ and $\boldsymbol{\beta}$ $(\boldsymbol{\beta} > \boldsymbol{\alpha})$ are the two greatest valence angles and $\boldsymbol{\theta}$ is the ideal tetrahedral angle (109.5°). The $\boldsymbol{\tau_4}$ and $\boldsymbol{\tau_4'}$ values for ideal square-planar and tetrahedral coordination spheres are 0 and 1, respectively. The calculated $\boldsymbol{\tau_4}$ and $\boldsymbol{\tau_4'}$ geometry indices are 0.07, 0.06 for **3a**, both 0.04 for **3c**, and 0.03, 0.02 for **3d**, respectively, pointing out a slightly distorted square-planar geometry.

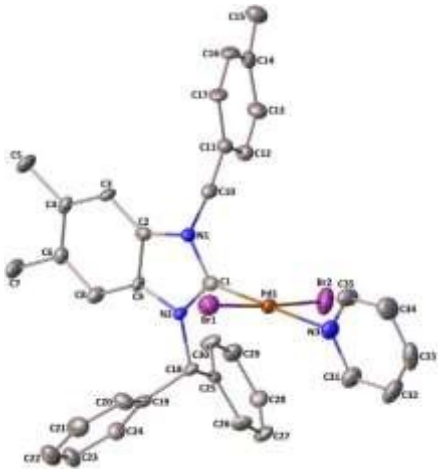

Figure 2. Molecular structure of **3a** drawn at 20% probability level. H atoms have been omitted for clarity.

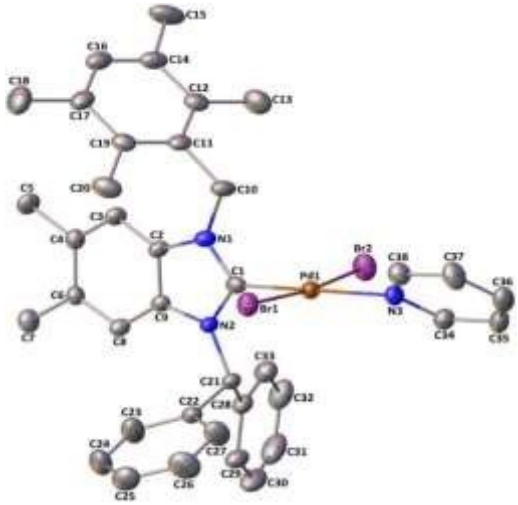

Figure 3. Molecular structure of **3b** drawn at 20% probability level. H atoms have been omitted for clarity.

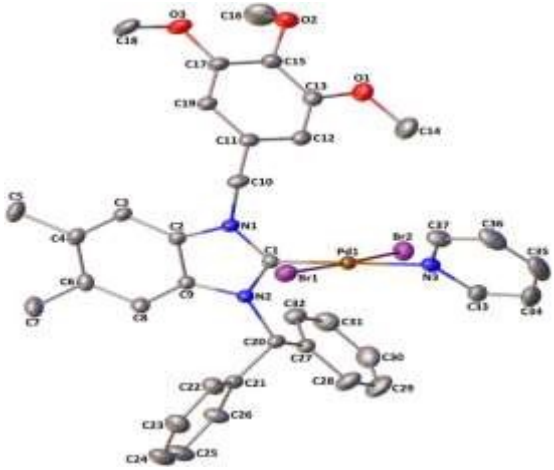

Figure 4. Molecular structure of **3d** drawn at 20% probability level. H atoms have been omitted for clarity.

View Article Online DOI: 10.1039/D1NJ03789C

Table 3. Selected distances (Å) and angles (°) for **3a, 3c** and **3e**

Parameters		Pd(II)-NHC complexes PEPPSI-Type 3a	3c	3e
Bond distances	Pd1–Br1	2.4281(9)	2.4182(16)	2.4339(5)
	Pd1–Br2	2.4102(10)	2.4352(15)	2.4052(5)
	Pd1–N3	2.127(6)	2.078(8)	2.111(3)
	Pd1–C1	1.965(8)	1.949(9)	1.964(3)
	N1–C1	1.353(9)	1.350(11)	1.349(4)
	N2–C1	1.341(9)	1.365(10)	1.346(5)
Bond angles (°)	Br1–Pd1–Br2	173.05(4)	175.95(6)	
	Br1–Pd1–N3	93.23(17)	91.7(2)	176.09(2)
	Br2–Pd1–N3	91.57(17)	91.1(2)	91.91(10)
	Br1–Pd1–C1	89.92(19)	90.1(2)	91.83(9)
	Br2–Pd1–C1	85.32(19)	87.0(2)	87.27(10)
	N3–Pd1–C1	176.8(2)	178.1(4)	88.99(10)
	N1–C1–N2	108.5(6)	107.1(7)	179.17(14)

The average Pd–C_{NHC} bond distance (1.96 Å) is smaller than the sum of the individual covalent radii of the palladium and carbon atoms (2.12 Å), while the average Pd–$N_{pyridine}$ bond distance (2.10 Å) is equal to the sum of the individual covalent radii of the palladium and nitrogen atoms (2.10 Å).[52] The Pd–Br distances are in the usual range, and the internal N–C–N ring angles at the carbene centers vary from 107.1(7) to 108.5(6)° in the complexes. In sum, these parameters are comparable with those observed for Pd-NHC-pyridine-Br_2 complexes.[53-59] The carbene ring is almost perpendicular to the coordination plane with a dihedral angle of 76.3(3)° in **3a**, 89.3(2)° in **3b** and 76.07(11)° in **3d**, which is typical for NHC complexes to reduce steric congestion. On the other hand, the dihedral angle between the pyridine ring and the coordination plane is 68.7(5)° in **3a**, 40.7(4)° in **3b**, and 51.8(2)° in **3d**.

Theoretical investigations

To gain further insights into the molecular structure and electronic properties of the synthesized complexes, DFT calculations at B3LYP/6-311G(d,p)/LANL2DZ level have been performed for complex **3a** as an example molecule. The obtained molecular geometry by DFT calculations was compared to that of X-ray analysis and the obtained results are shown in Figure 5. Some selected experimental and theoretical geometric parameters of complex **3a** are also reported in Table 4. As can be seen, the predicted molecular geometry of complex **3a** is strongly in agreement with the experimental results. The calculated Br1-Pb and Br2-Pb bond lengths were found to be 2.441 and 2.434 Å, respectively, which are in very good agreement with the experimental values (2.448 and 2.438 Å). The deviations between calculated and experimental angles for Br1-Pd-Br2 and Br1-Pd-N9 are only 0.02 and 0.01 respectively. The maximal discrepancies are found for the bond N8-Pd with a deviation of -0.249 Å, and the angles N8-Pd-C1 and Br1-Pd-C1 with deviations of 0.380° and 0.259°, respectively. These findings indicate that the DFT approach used is sufficiently accurate to predict the molecular geometry of complex **3a**.

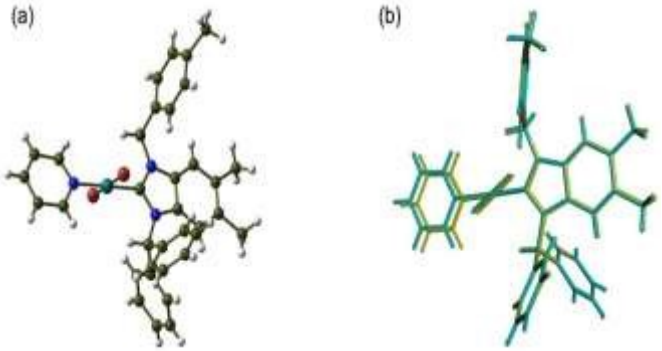

Figure 5. (a) The optimized molecular structure, and (b) atom-by-atom superimposition of the crystal structure (cyan) and the optimized molecular structure (yellow) of complex **3a.**

Table 4. Selected experimental and theoretical geometric parameters of complex **3a.**

Complex 3a	Calculated	Experimental	Discrepancy
Bond Distance (Å)			
N8-Pd	1.850	2.099	-0.249
Br1-Pb	2.441	2.448	-0.007
Br2-Pb	2.434	2.438	-0.004
C1-Pb	1.838	1.959	-0.121
C1-N1	1.346	1.364	-0.018
C1-N2	1.349	1.368	-0.019
Bond Angle (°)			
N8-Pd-C1	178.31	177.93	0.380
Br1-Pd-Br2	175.42	175.44	-0.020
Br1-Pd-C1	87.491	87.231	0.259
Br1-Pd-N9	90.836	90.840	-0.010

View Article Online
DOI: 10.1039/D1NJ03388C

ARTICLE

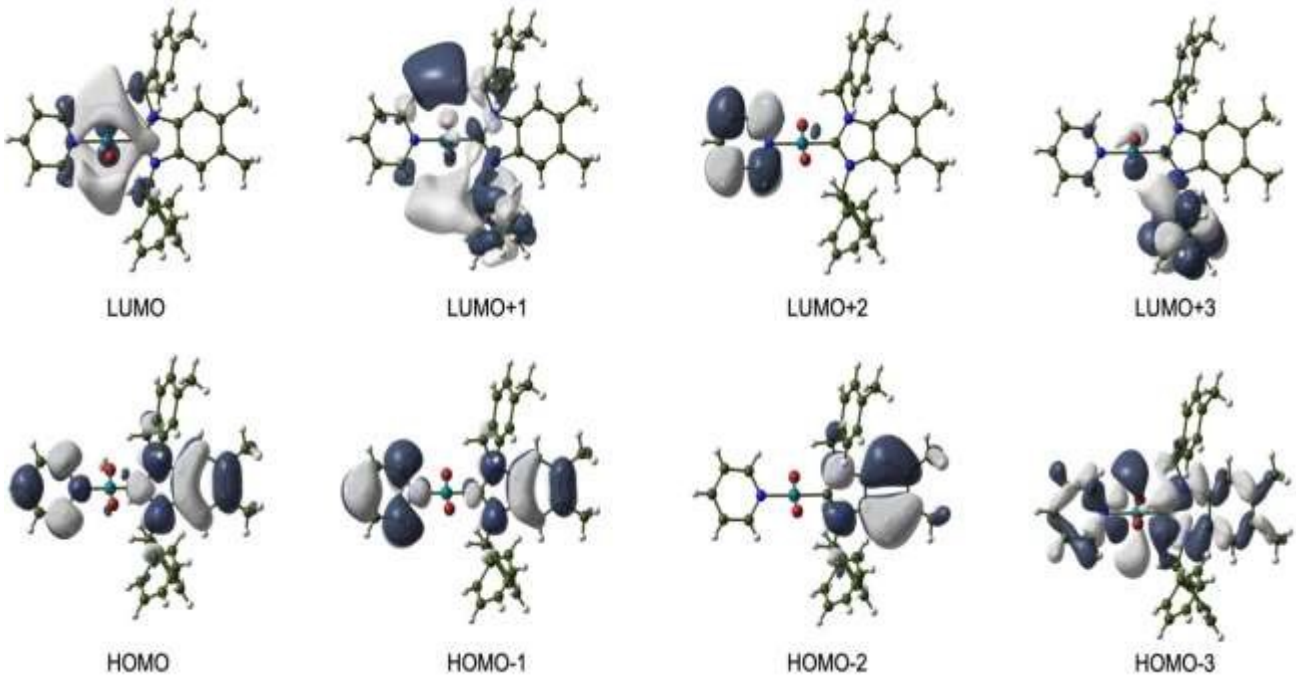

Figure 6. Frontier molecular orbitals of complex **3a** computed at B3LYP/6-311G(d,p)/ LANL2DZ level of theory.

Frontier molecular orbitals (FMOs), i.e. HOMO (Highest occupied molecular orbital) and LUMO (lowest unoccupied molecular orbital), are important parameters that could be used to characterize the stability and chemical reactivity of molecules.[60,61] The energy of HOMO is related to the electron donation ability, whereas that of LUMO represents the ability to accept electrons. The shape of FMOs could also give insights into the sites of electrophilic and nucleophilic attacks. The energy and distribution of FMOs, ranging from HOMO-3 to LUMO+3, of complex **3a**, have been calculated at B3LYP/6-311G(d,p)/LANL2DZ level and are reported in Figure 5 and Table 5, respectively. As illustrated in Table 5, the calculated FMOs energies are in the range of –0.43 to –5.91 eV. The difference between HOMO and LUMO energy (energy Gap) is only 2.26 eV, suggesting a high chemical reactivity of complex **3a**.[62,63] We can see also from Figure 6 that the HOMO and HOMO-1 are mainly distributed on the benzimidazole and the pyridine moieties with very small contributions of the Pd atom. HOMO-2 is located on the benzimidazole, while HOMO-3 is distributed on the benzimidazole, pyridine and Pd atom. These results indicate that the pyridine and the benzimidazole moieties are the most active sites for electron donation. Different from HOMOs which have relatively similar distributions, LUMOs of complex 3a is different. LUMO and LUMO+1 are mainly concentred on the metal center and the benzene ring for LUMO+1. The HOMO+2 is located on the pyridine ring, while LUMO+3 is distributed on the benzene rings and slightly on the Pd atom. These distributions of the electron density of HOMOs and LUMOs clearly show the transfer of the electron density from the benzimidazole and pyridine nucleus to the metal center and other regions of the molecule.

Molecular electrostatic potential (MEP) is another useful tool that can be used to describe the electronic properties and chemical reactivity of molecules.[64,65] MEP represents a 3D view of charge distributions within a molecule, color codes ranging from deep red for electron-rich sites to deep blue for electron-deficient sites are used. Figure 7 shows the MEP of complex **3a** calculated at B3LYP/6-311G(d,p)/ LANL2DZ level in the gas phase. The analysis of the obtained MEP reveals that the most electron-deficient sites of complex **3a** are located on the aromatic rings, in particular on the benzimidazole and pyridine. This suggests that these sites are the most suitable for nucleophilic attacks. On the other hand, the positive charges were found distributed on several aromatic hydrogen atoms and the metal center, indicating that these sites are the most electron-deficient and could be considered electrophilic sites.

View Article Online
DOI: 10.1039/D1NJ03388C

ARTICLE

Table 5. Energies in eV of the frontier molecular orbitals of complex **3a.**

Complex 3a	Energy in eV
LUMO+3	–0.43
LUMO+2	–0.73
LUMO+1	–0.87
LUMO	–1.22
HOMO	–3.48
HOMO-1	–4.21
HOMO-2	–5.79
HOMO-3	–5.91

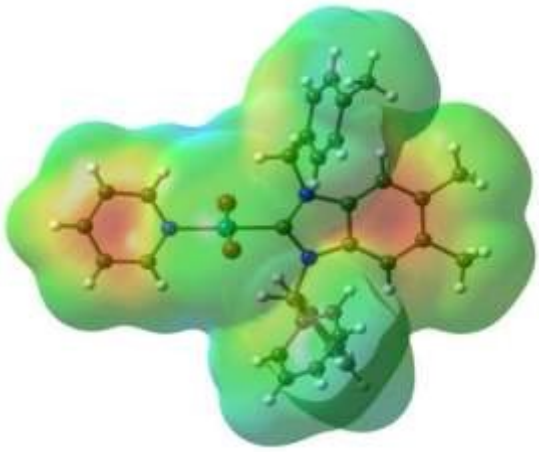

Figure 7. Molecular electrostatic potential (MEP) of complex **3a** computed at B3LYP/6-311G(d,p)/LANL2DZ level of theory.

Catalytic evaluation study

Optimization of the reaction conditions for the direct arylation of heteroaromatics with aryl bromides

The catalytic capacity of new Pd(II)-NHC complexes **3a-e** in intermolecular direct arylation reactions between aryl bromides and substituted furan, and thiophene derivatives were performed. As an attempt the first test was carried out at 120 °C for 24 h without Pd-catalyst, to examine the effect of catalyst, the reaction of 2-acetylfurane with bromobenzene was done in presence of KOAc as a base and dimethylacetamide (DMAc) as a solvent. The reaction didn't work and no desired product was formed. While in the same condition with the presence of 1 mol% Pd-catalyst complex, the reaction was working.

To optimize and determine the best reaction conditions of the direct arylation, we studied the reaction on changing (solvent, base, temperature, and time). Complex **3b** was selected as a model test catalyst, 2-acetylfurane as heteroaromatic substrates, and the *p*-bromobenzene as model coupling partner. As commonly used for the direct arylation of hetero-arenes, based on previous studies.[66,68] In this part, we start selected dimethylacetamide DMAc as a solvent, and potassium acetate KOAc as a base. Then we tried changing the time (1h, 2h, 4h) and temperature (80, 100, 120, 150°C) of the reaction. However, several attempts were made also with many solvents and bases for this study. The reactions were performed under argon. The results are summarized in Table 6.

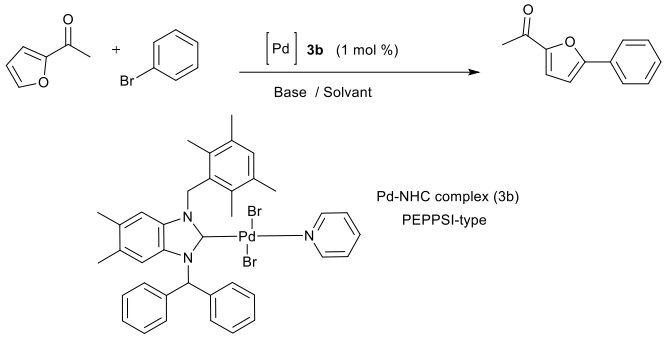

Scheme 2. Influence of the reaction conditions on the Pd-catalyzed direct arylation of five-membered heteroaromatics with *p*-bromobenzene

As shown in Table 6, The preliminary data demonstrated that the reaction displayed the best performance at 120°C temperature, and in a short time (1h) in presence of KOAc. When the reaction time was increased to 2 or 4 h, we observed full conversion, but no significant difference in yield. (Table 6, entries 7 and 10). When the temperature was increased from 120 °C, no noticeable effect on the yield was observed (Table 6, entry 4). When the temperature was reduced from 120 °C, low yields were observed (Table 6, entries 1 and 2). It was found also that DMAc was the best solvent among other solvents under the conditions tested. The evaluation of the effect of reaction temperature on yield at 150,120,100 and 80°C, gives the best yield at 120 °C. After fixing the first conditions of the reaction (time and temperature) with the successful results achieved in the optimization step. The evaluation of the reaction using various solvents and bases was carried out to confirm our coupling solvent/base choice. The test with different solvents as H_2O, EtOH, THF, Toluene, DMF, DMSO and dioxane was performed firstly in the presence of only 1 mol% **3b** catalyst, the reaction conversion was low with all solvent used, and

the yield was dropped to less than 10% (Table 6, entries 12-18). When the test was done with various bases such as K_2CO_3, KOH, TEA, and *t*-BuOK in the presence of only 1 mol% 3b catalyst. The reaction was working, but with low conversion and the final product was formed at lowest yields 5,7,6,9 % respectively (Table 6, entries 19-22). Therefore, DMAc and KOAc proved to be the best couple solvent/base in this reaction.

As a conclusion of these preliminary studies, it was observed that the best condition for direct arylation reaction using our Pd-catalysts complexes is 1h time, 120 °C temperature, and the couple DMAc/KOAc solvent/base.

Table 6. Optimization of the best conditions for direct arylation reaction

Entry	Solvent	Time (h)	Base	Temperature °C	Conversion (%)	Yield (%)
01				80	04	04
02		1	KOAc	100	63	23
03				120	95	86
04				150	95	75
05				80	04	04
06		2	KOAc	100	70	45
07				120	94	80
08	DMAc			150	96	81
16				80	95	82
09		4	KOAc	100	80	65
10				120	99	70
11				150	97	82
12	H_2O				06	05
13	EtOH				08	05
14	THF				02	01
15	Toluene	1	KOAc	120	10	09
16	DMF				09	06
17	DMSO				03	02
18	dioxane				04	03
19			K_2CO_3		10	05
20			KOH		14	09
21	DMAc	1	TEA	120	13	07
22			*t*-BuOK		11	06

The direct arylation of 2-acetylfuran, 2-acetylthiophene and furaldehyde with aryl bromides

Firstly, under the optimal condition, an investigation of the reactivity of 2-acetylfuran in Pd-catalyzed direct arylation with various (hetero)aryl bromides were carried out, a C(5)-arylated furane derivatives were obtained easily. The substate was coupling with eight *p*-substituted aryl bromides, (bromobenzene, *p*-bromotoluene, *p*-bromobenzaldehyde, *p*-bromoacetophenone, *p*- bromoanisole, 1-bromo-4-fluorobenzene, 1-bromo-4-(trifluoromethyl)benzene, and 3-bromoquinoline). Due to the Pd-catalyst, the reaction was perfectly working and the desired products were obtained with moderate to high yield, by using only 1 mol% Pd-complexes (3a-e) as a catalyst. The best yield was detected for the arylation with (hetero)aryl bromides which are poor of the electron as bromobenzene, *p*-bromotoluene, While the lowest yield was observed for electron-rich (hetero)aryl bromides as *p*-bromoacetophenone, *p*- bromoanisole. The preliminary studies showed that all Pd(II)-NHC complexes were active. The results of our experiments are summarized in Table 7. As shown in Table 7, an excellent conversion was observed with all Pd-catalysts, depending on the Pd(II) catalysts and the aryl bromides high-yield C(5)- arylated products were obtained for almost reactions. When 2-acetylfurane was arylated with bromobenzene, the products 5-phenyl-2-acetylfurane were obtained at 44-78% yields using Pd-complexes (**3a-e**) as a catalyst (Table 7, entries 1-5), the lowest yield was observed with Pd catalyst 3c, the reaction was working in 95-99% conversion. The same reaction of 2- acetylfurane with *p*-bromotoluene gave the desired product at 67-85% yield (Table 7, entries 6-10), and the conversion of the reaction was 89-99%. The reaction of 2- acetylfurane with *p*-bromobenzaldehyde gave the expected product with 64-91 yields (Table 7, entries 11-15), and with 99% conversion with all Pd-catalysts. The coupling with electron-poor *p*-bromoacetophenone was also given the expected product with a high yield at 71-82% and with 99 % conversion (Table 7, entries 16-20).

View Article Online
DOI: 10.1039/D1NJ03388C

Table 7. Direct C5-arylation of 2-acetylfuran with aryl bromides by using the new Pd-catalyst.

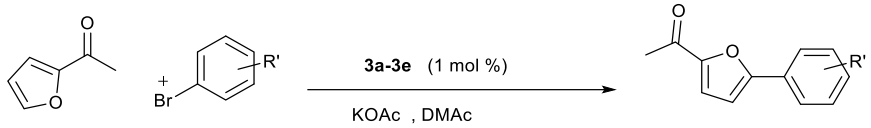

Entry	Aryl Bromide	[Pd]	Product	Conversion (%)	Yield (%)
1	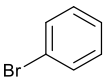	**3a**	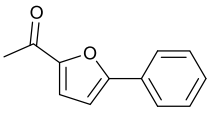	98	78
2		**3b**		95	67
3		**3c**		99	44
4		**3d**		99	72
5		**3e**		99	64
6	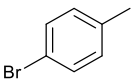	**3a**	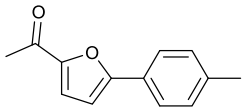	94	85
7		**3b**		98	73
8		**3c**		98	74
9		**3d**		89	67
10		**3e**		99	78
11	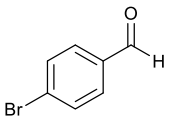	**3a**	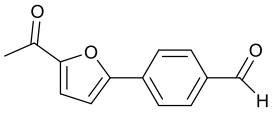	99	75
12		**3b**		99	64
13		**3c**		99	88
14		**3d**		99	85
15		**3e**		99	91
16	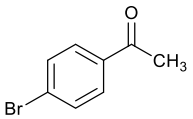	**3a**	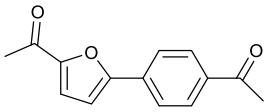	93	80
17		**3b**		99	71
18		**3c**		99	82
19		**3d**		99	72
20		**3e**		99	73
21	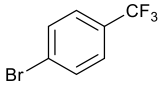	**3a**	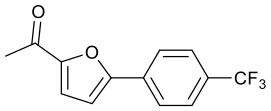	99	80
22		**3b**		99	70
23		**3c**		99	80
24		**3d**		99	82
25		**3e**		99	78
26	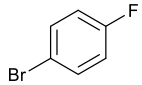	**3a**	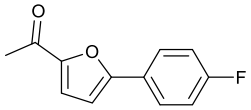	98	76
27		**3b**		99	74
28		**3c**		97	85
29		**3d**		99	76
30		**3e**		95	75
31	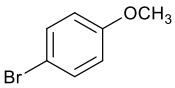	**3a**	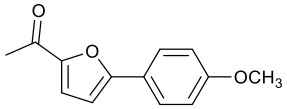	98	77
32		**3b**		77	62
33		**3c**		86	69
34		**3d**		81	43
35		**3e**		57	39
36	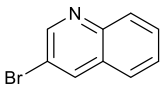	**3a**	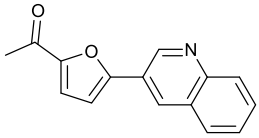	95	82
37		**3b**		97	80
38		**3c**		99	86
39		**3d**		93	84
40		**3e**		88	75

The reaction conditions: Pd catalyst (0.01 mmol), 2-acetylfuran (1.0 mmol), aryl bromide (1.0 mmol), KOAc (2 mmol), DMAc (2 mL), 120 °C and 1 h. GC yields were calculated concerning aryl bromide from the results of GC.

View Article Online
DOI: 10.1039/D1NJ03384C

The reaction of 2-acetylfurane with 1-bromo-4-(trifluoromethyl)benzene generated the 5-(4-trifluoromethyl)-2-acetylfurane at 70-86% yield and 99% conversion (Table 7, entries 21-25). The coubling with 1-bromo-4-fluorobenzene was given also a high yield at 74-85 (Table 7, entries 26-30) with 99% conversion. When the reaction was done with the *p*-bromoanisole, the obtained product formed with a moderate yield at 39-77%, and conversion between 57-99% (Table 7, entries 31-35). When the coupling was done with 3-bromoquinoline, the reaction gave a lower C5-arylated product with the lowest yield comparing with other reaction, the yield was observed between 8 % and 42% (Table 7, entries 36-40).

Using the same reaction conditions, The second test was performed, for the direct arylation of 2- acetylthiofene with the (hetero)aryl bromides used in the first test, C(5)-arylated thiophene derivatives were obtained. The arylation of 2-acetylthiophene was tested with a range of para-substituted aryl bromides wich were used in the first test, under the optimized conditions using all the Pd-catalysts. Due to these Pd-catalysts (**3a-e**), the reaction was perfectly working in 98-99% conversion with almost reaction tested, and the desired product was obtained at high yield in the average of 80%, the best yield was detected for the arylation with (hetero)aryl bromides which are poor of the electron as bromobenzene, *p*-bromotoluene. The results of this evaluation showed that all Pd(II)-NHC complexes PEPPSI-type were active catalysts. The results of these experiments are summarized in Table 8. As presented in Table 8, direct C5 arylation reactions resulted in moderate to high yields of desired coupling products. The excellent conversion was observed with all Pd-catalysts. When 2-acetylthiophene was arylated with bromobenzene, desired products were obtained at 78-93% yields using Pd-complexes (**3a-e**) as a catalyst (Table 8, entries 1-5), the reaction was working in 98% conversion. The same reaction of 2-acetylthiophene with p-bromotoluene gave the desired product at 84-92% yield (Table 8, entries 6-10), the conversion of the reaction was 92-98%. The reaction of 2- acetylthiophene with *p*-bromobenzaldehyde gave the expected product with 70-81 yields (Table 8, entries 11-15), with 99% conversion with almost Pd-catalysts. The coupling with electron-poor p-bromoacetophenone was also given the expected product with a high yield at 73-84% and with 93-99 % conversion (Table 8, entries 16-20). The reaction of 2-acetylthiophenene with 1-bromo-4-(trifluoromethyl)benzene generated the desired product at 60-94% yield and 65-98% conversion (Table 8, entries 21-55). Furthermore, 1-bromo-4-fluorobenzene was also successfully coupled with 2-acetylthiophene to give C5 arylated products in high yields at 86-95% (Table 8, entries 26-30) with 95-99% conversion. When the reaction was done with the p-bromoanisole, the obtained product formed with moderate to high yield at 56-82%, and conversion between 60-90% (Table 8, entries 31-35). When the coupling was done with 3-bromoquinoline, the reaction gave a good C5-arylated product with the same yield (80%) with all Pd-catalysts, the conversion o the reaction was 99 % (Table 8, entries 36-40).

The last evaluation of the new Pd-catalysts was performed, under the same condition, the direct arylation of 2- furaldehyde with the (hetero)aryl bromides which used in the first and second test, C(5)-arylated furaldehyde derivatives were obtained. The arylation of 2-furaldehyde was carried out using different p-substituted aryl bromides, (bromobenzene, *p*-bromotoluene, *p*-bromobenzaldehyde, *p*-bromoacetophenone, *p*-bromoanisole, and 3-bromoquinoline). Due to the Pd-catalyst (**3a-e),** the reaction was perfectly working and the desired product was obtained with moderate to high yield, the lowest yield was detected for the arylation with p- bromoanisole which is electron-rich. The results of this test showed that all Pd(II)-NHC complexes PEPPSI-type were catalytic active. The results of these experiments are summarized in Table 9.

As shown in Table 9, good results were observed with all Pd-catalysts, and high-to moderate yield C(5)- arylated products were obtained for almost all reactions. When 2-furaldehyde was arylated with bromobenzene, the products 5-phenyl-2-carbaldehyde were obtained at 46-86% yields using Pd-complexes (**3a**-**d**) as a catalyst, while the lowest yield (22%) was observed with Pd-catalyst **3e** (Table 9, entries 1-5), the reaction was working in 26-99% conversion. The same reaction of furaldehyde with *p*-bromotoluene gave the desired product at 51-82% yield (Table 9, entries 6-10), and the conversion of the reaction was 99%. The reaction of furaldehyde with *p*-bromobenzaldehyde gave the expected product with moderate yields at 53-65 (Table 9, entries 11-15), and with 78-99% conversion. The coupling with electron-poor *p*-bromoacetophenone was also given the expected product with a lower yield at 23-48% and with 27-71% conversion (Table 9, entries 16-20). The reaction of furaldehyde with 1-bromo-4-(trifluoromethyl)benzene generated the 5-(4-trifluoromethyl)-2-furaldehyde at 47-75% yield and 64-98% conversion (Table 9, entries 21-24), while the lowest yield was observed with the Pd-catalyst **3e** at 26%. The coupling with 1-bromo-4-fluorobenzene was given also a high yield at 55-85 (Table 9, entries 26-30) with 77-99% conversion. Relatively low yields were obtained for the coupling of furaldehyde with 4-bromoanisole, which an electron-rich aryl bromide, the obtained product formed at 09-16% (Table 9, entries 31-40). When the coupling was done with 3-bromoquinoline, the reaction gave a good C5-arylated product (Table 9, entries 36-40). Because pyridine derivatives such as quinolines are known π-electrondeficient heterocycles. Therefore, reactivity of these type compounds is quite similar to electron-deficient aryl bromides such as 4-bromoacetophenone [69]. Also as a result of this study, it was observed that the less active catalyst was **3e** complex at 22,28,26,16,55,37% yield (Table 9, entries 5,10,15,20,25,40)

View Article Online
DOI: 10.1039/D1NJ03388C

Table 8. Direct C5-arylation of 2-acetylthiophene with aryl bromides by using the new Pd-catalyst.

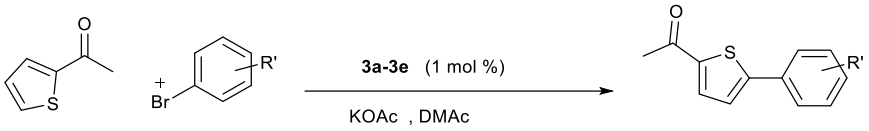

Entry	Aryl Bromide	[Pd]	Product	Conversion (%)	Yield (%)
1	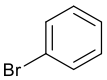	**3a**	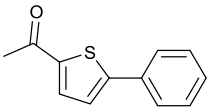	98	78
2		**3b**		98	93
3		**3c**		99	93
4		**3d**		98	92
5		**3e**		98	93
6	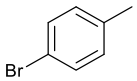	**3a**	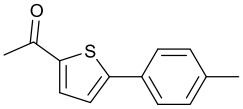	92	86
7		**3b**		96	92
8		**3c**		98	84
9		**3d**		95	89
10		**3e**		95	89
11	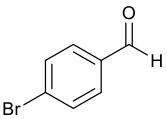	**3a**	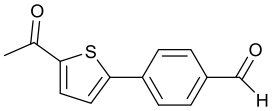	99	70
12		**3b**		98	75
13		**3c**		99	81
14		**3d**		99	80
15		**3e**		99	81
16	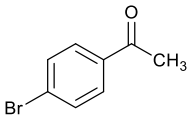	**3a**	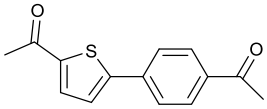	99	77
17		**3b**		96	84
18		**3c**		94	75
19		**3d**		98	82
20		**3e**		93	73
21	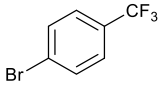	**3a**	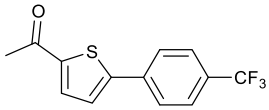	77	75
22		**3b**		98	94
23		**3c**		65	60
24		**3d**		90	85
25		**3e**		90	85
26	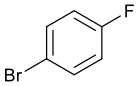	**3a**	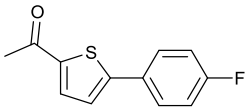	99	95
27		**3b**		97	93
28		**3c**		97	94
29		**3d**		96	90
30		**3e**		95	86
31	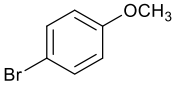	**3a**	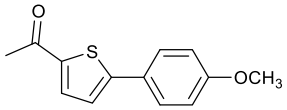	90	80
32		**3b**		60	56
33		**3c**		82	74
34		**3d**		67	60
35		**3e**		90	82
36	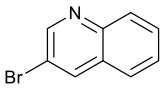	**3a**	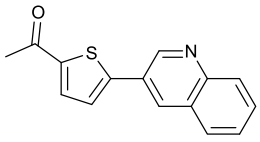	99	80
37		**3b**		99	80
38		**3c**		99	80
39		**3d**		99	80
40		**3e**		99	79

The reaction conditions: Pd catalyst (0.01 mmol), 2-acetylthiophene (1.0 mmol), aryl bromide (1.0 mmol), KOAc (2 mmol), DMAc (2 mL), 120 °C and 1 h. GC yields were calculated concerning aryl bromide from the results of GC.

View Article Online
DOI: 10.1039/D1NJ03388C

Table 9. Direct C5-arylation of 2-furaldeyde with aryl bromides by using the new Pd-catalyst.

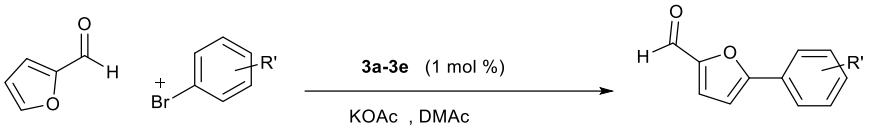

Entry	Aryl Bromide	[Pd]	Product	Conversion (%)	Yield (%)
1	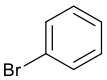	**3a**	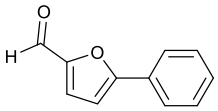	99	86
2		**3b**		99	90
3		**3c**		98	76
4		**3d**		50	46
5		**3e**		26	22
6	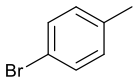	**3a**	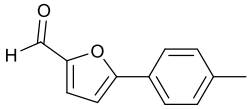	99	76
7		**3b**		98	79
8		**3c**		99	82
9		**3d**		98	51
10		**3e**		99	82
11	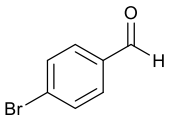	**3a**	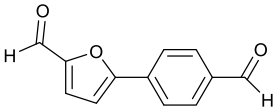	99	65
12		**3b**		93	63
13		**3c**		99	65
14		**3d**		78	53
15		**3e**		94	63
16	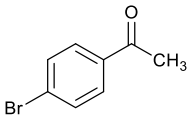	**3a**	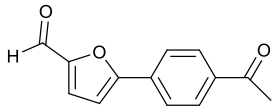	35	27
17		**3b**		27	23
18		**3c**		71	46
19		**3d**		66	47
20		**3e**		41	28
21	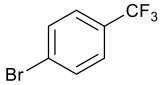	**3a**	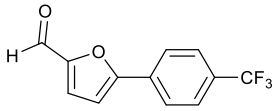	98	75
22		**3b**		79	59
23		**3c**		65	50
24		**3d**		64	47
25		**3e**		29	26
26	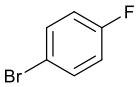	**3a**	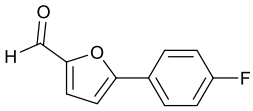	99	82
27		**3b**		99	85
28		**3c**		99	72
29		**3d**		99	70
30		**3e**		74	55
31	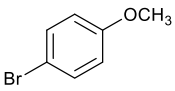	**3a**	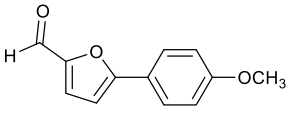	13	09
32		**3b**		11	09
33		**3c**		13	10
34		**3d**		11	10
35		**3e**		19	16
36	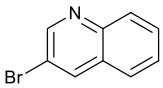	**3a**	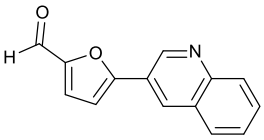	99	74
37		**3b**		75	48
38		**3c**		93	77
39		**3d**		69	47
40		**3e**		55	37

The reaction conditions: Pd catalyst (0.01 mmol), 2-furaldeyde (1.0 mmol), aryl bromide (1.0 mmol), KOAc (2 mmol), DMAc (2 mL), 120 °C and 1 h. GC yields were calculated concerning aryl bromide from the results of GC.

View Article Online
DOI: 10.1039/D1NJ03388C

Conclusions

In summary, a new series of PEPPSI-type palladium-NHC complexes (**3a-e**) based benzimidazole group were prepared using 5,6-dimethylbenzimidazolium salts with $PdCl_2$ in pyridine to give a new Pd-catalysts. All Pd(II)-NHC complexes were successfully characterized by spectroscopic analytical methods. Further, the crystal structures of **3a**, **3b**, and **3d** Pd-*N*HC complexes were also reported. Theoretical calculations using DFT/B3LYP approach have been performed to gain further insights into the molecular structure and electronic properties of complex **3a**. The catalytic activities of these Pd(II)-NHC complexes were investigated in the direct C(5)-arylation of C(2)-blocked as 2-acetylfuran, 2-acetylthiophene, and 2-furaldehyde. In most cases, high yields were observed using only 1 mol% catalyst of Pd-catalyst with all complexes in a very short time (1h). All of these Pd(II)-NHC complexes were found to be suitable for the arylation reaction of aryl bromide with heteroaromatics. Moreover, thiophene and furan derivatives can be efficiently and selectively arylated at the C(5)-position. Satisfactory results were obtained as compared with previously reported similar studies. All new PEPPSI-type palladium-NHC complexes (**3a-e**) proved to be active in the direct arylation reaction. In addition, it was seen that the reaction conditions were more moderate in terms of reaction temperature, time, and quantity of catalyst amount.

Author Contributions

Abd el-Krim Sandeli: Investigation; Naima Khiri-Meribout: Supervision, Writing –Review and Editing; Saida Benzerka: Formal analysis; Houssem Boulebd: Formal analysis; Nevin Gürbüz: Investigation, Visualization; Namık Özdemir: Formal analysis; İsmail Özdemir: Resources, Funding acquisition, Writing-Review and Editing.

Conflicts of interest

There are no conflicts to declare.

Acknowledgements

The authors greatly acknowledge financial support from the İnönü University Research Fund (İÜ-BAP: FBG-2019-1594) of this work. X-ray study was supported by the Scientific Research Projects Unit of Ondokuz Mayıs University (Project No: PYO.FEN.1906.19.001).

Appendix A. Supplementary data

CCDC 2073777, 2073779, 2073780 contains the supplementary crystallographic data for the compounds reported in this article. These data can be obtained free of charge on application to CCDC, 12 Union Road, Cambridge CB2 1EZ, UK [Fax: +44 1223 336 033, e-mail: deposit@ccdc.cam.ac.uk, https://www.ccdc.cam.ac.uk/structures/]. All the supplementary data (^{1}H, ^{13}C-NMR, and Crystallographic data) are given in supplementary information

Notes and references

1 A. J. Arduengo III, R. L. Harlow, and M. Kline, *J. Am. Chem. Soc.* 1991, **113**, 361-363.
2 F. Glorius, N-heterocyclic carbenes in transition metal catalysis, vol. 21. Springer, 2007.
3 M. G. Organ, G. A. Chass, D.-C. Fang, A. C. Hopkinson, and C. Valente, *Synthesis*, 2008, **17**, 2776-2797.
4 C. C. C. Johansson Seechurn, M. O. Kitching, T. J. Colacot, and V. Snieckus*, Angew. Chem. Int. Ed.*, 2012, **51**, 5062–5085.
5 W. A. Herrmann, *Angew. Chem. Int. Ed.*, 2002, **41**, 1290–1309.
6 N. Gürbüz, E. Ö. Karaca, İ. Özdemir, B. Cetinkaya, *Turkish J. Chem*., 2015, **39**, 1115–1157.
7 E. A. B. Kantchev, C. J. O'Brien, and M. G. Organ, *Angew. Chem. Int. Ed.*, 2007, **46**, 2768–2813.
8 F. Bellina and R. Rossi, *Chem. Rev*., 2010, **110**, 1082–1146.
9 Y. Akita, A. Inoue, K. Yamamoto, A. Ohta, and T. Kurihara, *Heterocycles*, 1985, **23**, 2327–2333.
10 A. Ohta, Y. Akita, T. Ohkuwa, M. Chiba, and R. Fukunaga, *Heterocycles*, 1990, **31**, 1951–1958.
11 Y. Aoyagi, A. Inoue, R. Honma, Y. Akita, and A. Ohta, *Heterocycles*, 1992, **33**, 257–272.
12 N. Marion and S. P. Nolan, *Acc. Chem. Res*., 2008, **41**, 1440–1449.
13 X.-X. He, Y. Li, B.-B. Ma, Z. Ke, and F.-S. Liu, *Organometallics*, 2016, 35, 2655–2663.
14 M. Kaloğlu, İ. Özdemir, V. Dorcet, C. Bruneau, and H. Doucet, *Eur. J. Inorg. Chem*., 2017, **2017**, 1382–1391.
15 H. Lv, L. Zhu, Y. Tang, and J. Lu, *Appl. Organomet. Chem*., 2014, **28**, 27–31.
16 W. Sikorski, W. Zawartka, and A. M. Trzeciak, *J. Organomet. Chem*., 2018, **867**, 323–332.
17 S. Karthik and T. Gandhi, *Org. Lett.*, 2017, **19**, 5486–5489.
18 M. Ionita, J. Roger, and H. Doucet, *ChemSusChem*, 2010, **3**, 367–376.
19 A. L. Gottumukkala and H. Doucet, *Eur. J. Inorg. Chem.* 2007, 3629–3632.
20 P. Xi, F.Yang, S. Qin, D. Zhao, J. Lan, G. Gao, C. Hu and J. You, *J. Am. Chem. Soc.,* 2010, **132**,1822–1824.
21 T. Satoh and M. Miura, *Chem. Lett*., 2007, **36**, 200–205.
22 S. Yang, C. Sun, Z. Fang, B. Li, Y. Li, and Z. Shi, Angew. Chem., 2008, **120**, 1495–1498.
23 L. Chen, J. Roger, C. Bruneau, P. H. Dixneuf, and H. Doucet, *Chem. Commun*., 2011, **47**, 1872–1874.
24 M. Nakano, H. Tsurugi, T. Satoh, and M. Miura, *Org. Lett*., 2008, **10**, 1851–1854.
25 E. Üstün, Ş. Koç, S. Demir, and İ. Özdemir, *J. Organomet. Chem.* 2016, **815**, 16–22.
26 E. Üstün, A. Özgür, K. A. Coşkun, S. D. Düşünceli, İ. Özdemir, and Y. Tutar, *Transit. Met. Chem*., 2017, **42**, 331–337.
27 G. Onar, C. Gürses. M. O. Karataş, S. Balcıoğlu, N. Akbay, N. Özdemir, B. Ateş and B. Alıcı, *J. Organomet. Chem*., 2019, **886**, 48–56.
28 E. Peris and R. H. Crabtree, *Coord. Chem. Rev*., 2004, **248**, 2239–2246.

29 S. P. Nolan, N-Heterocyclic carbenes in synthesis. John Wiley & Sons, 2006.
30 Y. Borguet, G. Zaragoza, A. Demonceau, and L. Delaude, *Dalton Trans*., 2013, **42**, 7287–7296.
31 A. Beladhria, A. L.Gottumukkala, C. Youssef, C. B. Bheeter, H. Ben Ammar, R. Ben Salem and H. Doucet *Cat. Commun*., 2013, **41**, 119–122.
32 I. Smari, C. Youssef, H. Ben Ammar, B. Ben Hassine, J.-F. Soulu, and H. Doucet, *Tetrahedron*, 2015, **71**, 6586–6593.
33 E. C. Chao, *Drugs Future*, 2011, 36, 351–357.
34 A.-K. Sandeli, N. Khiri-Meribout, S. Benzerka, N. Gürbüz, M. Dündar, H. Karcı, C. Bensouici, El H. Mokrani, İ. Özdemir, A. Koç, N. Özdemir, A. Debache and İ.Özdemir, *Inorg. Chim. Acta*, 2021, 525, 120486-120499.
35 S. Cie, "X-area (version 1.18) and X-red32 (version 1.04)," Darmstadt, Germany, 2002.
36 L. Palatinus and G. Chapuis*, J. Appl. Crystallogr*., 2007, **40**, 786–790.
37 D. Kratzert, J. J. Holstein, and I. Krossing, *J. Appl. Crystallogr*., 2015, **48**, 933–938.
38 O. V Dolomanov, L. J. Bourhis, and R. J. Gildea, J. *Appl. Crystallogr*., 2009, **42**, 339–341.
39 R. A. Gaussian09, Inc., Wallingford CT, 2009, *121*, 150–166.
40 P. C. Hariharan and J. A. Pople, *Theor. Chim. Acta*, 1973, **28**, 213–222.
41 A. D. Becke, *Phys. Rev. A*,1988, **38**, 3098.
42 P. J. Hay and W. R. Wadt, *Int. J. Chem. Phys*., 1985, 82, 270–283.
43 A. D. McLean and G. S. Chandler*, Int. J. Chem. Phys*., 1980, **72**, 5639–5648.
44 J. Tirado-Rives and W. L. Jorgensen, *J. Chem. Theory Comput*., 2008, **4**, 297–306.
45 I. A. Khodja, H. Boulebd, C. Bensouici, and A. Belfaitah, *J. Mol. Struct*., 2020, **1218**, 128527.
46 I. A. Khodja and H. Boulebd, *Mol. Divers.*, 2020, 1–12.
47 M. Kaloğlu and İ. Özdemir, *Appl. Organomet. Chem*., 2018, **32**, e4399.
48 H. A. Chiong and O. Daugulis, *Org. Lett*., 2007, **9**, 1449–1451.
49 İ. Özdemir, Y. Gök, Ö. Özeroğlu, M. Kaloğlu, H. Doucet and C. Bruneau, *Eur. J. Inorg. Chem*., 2010, 1798-1805.
50 L. Yang, D. R. Powell, and R. P. Houser, *Dalton Trans*. 2007, **9**, 955–964.68
51 A. Okuniewski, D. Rosiak, J. Chojnacki, and B. Becker, *Polyhedron*, 2015, **90**, 47–57.
52 B. Cordero, V. Gómez, Ana E. Platero-Prats, M. Revés, J. Echeverría, E. Cremades, F. Barragána and S. Alvarez, Dalton Trans. 2008, 2832–2838.
53 Y. Han, H. V. Huynh, and G. K. Tan, *Organometallics*, 2007, **26**, 6447–6452.
54 H. V. Huynh, W. Sim, and C. F. Chin, Dalton Trans., 2011, **40**, 11690–11692.
55 Y.-C. Lin, H.-H. Hsueh, S. Kanne, L.-K. Chang, F.-C. Liu, I. J. B. Lin, G.-H. Lee and S.-M. Peng, *Organometallics*, 2013, **32**, 3859–3869.
56 L. Barbu, M. M. Popa, S. Shova, M. Ferbinteanu, C. Draghici, and F. Dumitrascu*, Inorg. Chim. Acta*, 2017, **463**, 97–101.
57 N. Kaloğlu, M. Kaloğlu, M.N. Tahir, C. Arıcı, C. Bruneau, H. Doucet, P. H. Dixneuf, B. Cetinkaya and İ. Özdemir, J. *Organomet. Chem.,* 2018, **867**, 404–412.
58 M. Kaloğlu, N. Kaloğlu, İ. Yıldırım, N. Özdemir, and İ. Özdemir, *J. Mol. Struct*., 2020, **1206**, 127668-127679.
59 M. Kaloğlu, N. Gürbüz, İ. Yıldırım, N. Özdemir, and İ. Özdemir, *Appl. Organomet. Chem*., 2020, **34**, p. e5387.
60 H. Boulebd, Y. D. Lahneche, I. A. Khodja, M. Benslimane, and A. Belfaitah, *J. Mol. Struct*., 2019, **1196**, 58–65.
61 A. Nataraj, V. Balachandran, and T. Karthick, *J. Mol. Struct*., 2013, **1038**, 134–144.
62 M. Kumar, M. Kariem, H. N. Sheikh, A. Frontera, S. K. Seth, and A. K. Jassal, *Dalton Trans*., 2018, **47**, 12318–12336.
63 Y.-Y. Cai, L.-Y. Xu, L.-Q. Chai, and Y.-X. Li, *J. Mol. Struct*., 2020, **1204**, 127552-127561.
64 H. Boulebd, *Free Radic. Res*., 2020, **54**, 221–230.
65 H. Boulebd, *Phytochemistry,* 2021, 184, 112670-112677.
66 E. David, C. Rangheard, S. Pellet-Rostaing, and M. Lemaire, *Synlett*, 2006, **2006**, 2016–2020.
67 E. O. Karaca, N. Gürbüz, İ. Özdemir, H. Doucet, O. Şahin, O. Büyükgüngör and B. Çetinkaya, *Organometallics*, 2015, vol. **34**, no. 11, pp. 2487–2493.
68 E. David, S. Pellet-Rostaing, and M. Lemaire, *Tetrahedron*, 2007, **63**, 8999–9006.
69 Y. Fall, C. Reynaud, H. Doucet and M. Santelli, *Eur. J. Org. Chem.* 2009, **24**, 4041–4050.